SAND2000-1869C

GaN HIGH POWER DEVICES

S.J. Pearton,[1] F. Ren,[2] A.P. Zhang,[2] G. Dang,[2] X.A. Cao,[7] K.P. Lee,[1] H. Cho,[1] B.P. Gila,[1] J.W. Johnson,[2] C. Monier,[1] C.R. Abernathy,[1] J. Han,[4] A.G. Baca,[4] J.-I. Chyi,[5] C.-M. Lee,[5] T.-E. Nee,[5] C.-C. Chuo,[5] G.C. Chi[6] and S.N.G. Chu[7]

[1] Department of Materials Science and Engineering, University of Florida, Gainesville, FL 32611, USA
[2] Department of Chemical Engineering, University of Florida, Gainesville, FL 32611, USA
[3] Department of Materials Engineering, Miryang National University, Kyungnam, Korea
[4] Sandia National Laboratories, Albuquerque, NM 87185, USA
[5] Department of Electrical Engineering, National Central University, Chung-Li, 32054, Taiwan
[6] Department of Physics, National Central University, Chung-Li, 32054, Taiwan
[7] Bell Laboratories, Lucent Technologies, Murray Hill, NJ 07974, USA

ABSTRACT

A brief review is given of recent progress in fabrication of high voltage GaN and AlGaN rectifiers, GaN/AlGaN heterojunction bipolar transistors, GaN heterostructure and metal-oxide semiconductor field effect transistors. Improvements in epitaxial layer quality and in fabrication techniques have led to significant advances in device performance

INTRODUCTION

Ultra-high Power Switches

There is a strong interest in developing wide bandgap power devices for use in the electric power utility industry. With the onset of deregulation in the industry, there will be increasing numbers of transactions on the power grid in the US, with different companies buying and selling power. The main applications are in the primary distribution system (100-2000 kVA) and in subsidiary transmission systems (1-50MVA). A major problem in the current grid is momentary voltage sags, which affect motor drives, computers and digital controls. Therefore, a system for eliminating power sags and switching transients would dramatically improve power quality. For example it is estimated that a 2-second outage at a large computer center can cost $600,000 or more, and an outage of less than one cycle, or a voltage sag of 25% for two cycles, can cause a microprocessor to malfunction. In particular,

DISCLAIMER

computerized technologies have led to strong consumer demands for less expensive electricity, premium quality power and uninterruptible power.

The basic power electronics hierarchy would include the use of widegap devices such as Gate Turn-Off Thyristors (GTOs), MOS-Controlled Thyristors (MCT) or Insulated Gate Bipolar Transistors (IGBTs) combined with appropriate packaging and thermal management techniques to make subsystems (such as switches, rectifiers or adjustable speed devices) which then comprise a system such as Flexible AC Transmissions (FACTS). Common power electronics systems, which are inserted between the incoming power and the electrical load include uninterruptible power supplies, advanced motors, adjustable speed drives and motor controls, switching power supplies, solid-state circuit breakers and power conditioning equipment. About 50% of the electricity in the US is consumed by motors. Motor repairs cost ~$5B each year and could be dramatically reduced by high power electronic devices that permit smoother switching and control. Moreover, control electronics could dramatically improve motor efficiency. Other end uses include lighting, computers, heating and air-conditioning.

The FACTS concept employed in electricity transmission aims for the following:

- Precisely regulate power flow on particular lines.
- Better system stability by instantly counteracting transients.
- Load transmission lines closer to their thermal limits (increase capacity) using:

• Thyristor controlled series capacitor (changes line impedance).
• Static compensator (STATCOM based on GTO thyristors) provides voltage support on lines by generating or absorbing reactive power without need for large external reactors or capacitor banks and mitigates disturbances.
• United Power Flow Controller (comprehensively controls power flow, reduces line impedance, shifts phase angle, provides voltage support).

On the distribution side there is a need to precisely manage power quality and flow for variable loads. The components include the dynamic static compensator (DSTATCOM), which protects the line from a "dirty" load (and generally involves Si IGBTs), the dynamic voltage restorer, which protects a sensitive load from line disturbances (and also employs Si IGBTs) and solid-state breaker/transfer switches, which prevent black-outs (and employ semiconductor-controlled rectifiers and GTOs).

Thus the technology drivers for high power semiconductor devices from the utility viewpoint are:

- FACTS (Flexible AC Transmission System) Devices that allow power grids to be tuned for maximum performance like low-power integrated circuits, increasing asset utilization.
- Distribution system components that enable precise subcycle regulation of voltage and power flow, including solid-state transfer switch (SSTS), solid-state circuit breaker (SSCB), dynamic voltage restorer (DVR), static compensator (D-STATCOM), advanced transformer, fault current limiter.

- Power electronics interconnection technologies (ac/dc inverters, frequency changers) that enable wider application of low- and no-emission systems for energy generation and storage including fuel cells, wind power, photovoltaics, batteries and superconducting magnetic energy storage.
- Advanced motor speed controllers that reduce or eliminate the significant power disturbances produced by existing adjustable speed drive.
- Power management technologies for electric vehicles that reduce pollution and dependence on imported oil.

Other high-power electronics applications include hybrid drivetrain (electric) vehicles, next generation ("all-electric") battleships and the "more-electric" airplane for both military and commercial deployment.

Some desirable attributes of next generation, widegap power electronics include the ability to withstand currents in excess of 5 kA and voltages in excess of 50 kV, provide rapid switching, maintain good thermal stability while operating at temperatures above 250°C, have small size and light-weight, and be able to function without bulky heat-dissipating systems.

The primary limits of Si-based power electronics are:

(i) Maximum voltage ratings <7 kV

- Multiple devices must be placed in series for high-voltage systems.

(ii) Insufficient current-carrying capacity

- Multiple devices must be placed in parallel for typical power grid applications.

(iii) Conductivity in one direction only

- Identical pairs of devices must be installed in anti-parallel for switchable circuits.

(iv) Inadequate thermal management

- Heat damage is a primary cause of failure and expense.

(v) High initial cost

- Applications are limited to the highest-value settings.

(vi) Large and heavy components

- Costs are high for installation and servicing, and equipment is unsuitable for many customers.

For these reasons, there is a strong development effort on widegap power devices, predominantly SiC, with lesser efforts in GaN and diamond, which should have benefits that Si-based or electromechanical power electronics cannot attain. The higher stand-off voltages should eliminate the need for series stacking of devices and the associated packaging difficulties. In addition these widegap devices should have higher switching frequency in pulse-width-modulated rectifiers and inverters.

The current state-of-the-art in Si power devices includes 6" diameter light-triggered thyristors rated at 8 kV, 3.5 kA average current, GTO thyristors rated at 6 kV and 2kA in practical applications and press-pack reverse-conducting IGBTs rated at 2.5 kV and 1 kA.

Light triggering is often needed in stacked devices to ensure all of them turn-on at the same time. This might be used to advantage in power grid applications in another way, namely that control signals could be carried on the extensive optical fiber network that accompanies the power grid, and could be used to trigger GaN-based devices. Moreover, Er-doped GaN emitters could be used to send status signals back through the same network.

The absence of Si devices capable of application to 13.8 kV distribution lines (a common primary distribution mode) opens a major opportunity for widegap electronics. However cost will be an issue, with values of $200-2000 per kVA necessary to have an impact. It is virtually certain that SiC switches will become commercially available within 3-5 years, and begin to be applied to the 13.8 kV lines. MOS Turn-Off-Thyristors involving a SiC GTO and SiC MOSFET are a promising approach. An inverter module can be constructed from an MOS turn-off thyristor (MTO) and a SiC power diode.

Bandic et al. predict that a 5 kV stand-off voltage can be supported by a 20 μm $Al_{0.2}Ga_{0.8}N$ layer doped at ~$10^{16}cm^{-3}$. One of the questions marks about the GaN/AlGaN system is whether because they are direct gap materials and have extremely short minority-carrier lifetimes, that thyristors will not be possible due to an inability to build up sufficient charge in thick drift layers. At Al concentrations >0.5, the AlGaN is indirect, but little information is available on lifetimes in the material. As a first step to building these devices, Ren et al. recently demonstrated a GaN/AlGaN HBT capable of operation at ≥300°C.

Packaging and thermal management will be a key part of future power devices. For current Si IGBTs, there are two basic package types – the first is a standard attached die, wire bond package utilizing soft-solder and wire-bonds as contacts, while the second is the presspack, which employs dry-pressed contacts for both electrical and thermal paths. In the classical package the IGBTs and control diodes are soldered onto ceramic substrates, such as AlN, which provide electrical insulation, and this in turn is mounted to a heat sink (typically Cu). Thick Al wires (500 μm) are used for electrical connections, while silicone gel fills the package. In the newer presspack style, the IGBT and diode are clamped between Cu electrodes, buffered by materials such as molybdenum or composites whose purpose is to account for the thermal expansion coefficient differences between Si and Cu. The package is again filled with gel for electrical insulation and corrosion resistance.

There are numerous advantages of the AlGaInN system for high power electronics, including wide bandgaps for high voltage and temperature operation, good transport properties, the availability of heterostructures and finally the experience base accumulated during the development of nitride-based light-emitting diodes and lasers. Most of the work on nitride-based electronics has focused on AlGaN/GaN high electron mobility transistors for power microwave applications [1-6], but there are potential advantages to the use of bipolar transistors (either heterojunction bipolar transistors or bipolar junction transistors) in some applications because of their higher current densities, better linearity and more uniform threshold voltages. GaN/AlGaN bipolar transistors are an attractive option for various

satellite, radar and communications applications in the 1-5 GHz frequency range, at temperatures >400°C and powers >100 Watts. Traditional Si-based technologies cannot support such requirements, but the wide bandgap GaN materials system is capable of reaching this performance level. A summary of progress in GaN electronics is given in Table I.

In addition there is a strong interest in developing high current, high voltage switches in the AlGaN materials system for applications in the transmission and distribution of electric power and in the electrical sub-systems of emerging vehicle, ship and aircraft technology. It is expected that packaged switches made from AlGaN may operate at temperatures in excess of 250°C without liquid cooling, thereby reducing system complexity, weight and cost. In terms of voltage requirements, there is a strong need for power quality enhancement in the 13.8kV class, while it is estimated that availability of 20-25 kV switches in a single unit would cause a sharp drop in the cost of power flow control circuits. Schottky and p-i-n rectifiers are an attractive vehicle for demonstrating the high voltage performance of different materials systems and blocking voltages from 3-5·9 kV have been reported in SiC devices. The reverse leakage current in Schottky rectifiers is generally far higher than expected from thermionic emission, most likely due to defect states around the contact periphery. To reduce this leakage current and prevent breakdown by surface flash-over, edge termination techniques such as guard rings, field plates, beveling or surface ion implantation are necessary. However in the few GaN rectifiers reported so far, there has been little effort on employing edge termination methods and no investigation of the effect of increasing the bandgap by use of AlGaN.

In this paper we will detail recent results in GaN power electronic devices, including Schottky rectifiers, HBTs, BJTs, MOSFETs and HEMTs. The pace of advancement of these technologies has been remarkably rapid in the past 2 years.

GaN RECTIFIERS

For these devices, the GaN was grown on c-plane Al_2O_3 substrates by Metal Organic Chemical Vapor Deposition using trimethylgallium and ammonia as the precursors. For vertically-depleting devices, the structure consisted of a 1μm n^+ ($3x10^{18}$ cm^{-3}, Si-doped) contact layer, followed by undoped ($n=2.5x10^{16}$ cm^{-3}) blocking layers which ranged from 3-11μm thick. These samples were formed into mesa diodes using Inductively Coupled Plasma etching with Cl_2/Ar discharges (300 W source power, 40 W rf chuck power). The dc self-bias during etching was –85 V. To remove residual dry etch damage, the samples were annealed under N_2 at 800°C for 30 secs. Ohmic contacts were formed by lift-off of e-beam evaporated Ti/Al, annealed at 700°C for 30 secs under N_2 to minimize the contact resistance. Finally, the rectifying contacts were formed by lift-off of e-beam evaporated Pt/Au. Contact diameters of 60-1100μm were examined.

Table I. Historical development of GaN-based electronics.

Year	Event	Authors
1969	GaN by hydride vapor phase epitaxy	Maruska and Tietjen
1971	MIS LEDs	Pankove et al.
	GaN by MOCVD	Manasevit et al.
1974	GaN by MBE	Akasaki and Hayashi
1983	AlN intermediate layer by MBE	Yoshida et al.
1986	Specular films using AlN buffer	Amano et al.
1989	p-type Mg-doped GaN by LEEBI and GaN p-n junction LED	Amano et al.
1991	GaN buffer layer by MOCVD	Nakamura
1992	Mg activation by thermal annealing	Nakamura et al.
	AlGaN/GaN two-dimensional electron gas	Khan et al.
1993	GaN MESFET	Khan et al.
	AlGaN/GaN HEMT	Khan et al.
	Theoretical prediction of piezoelectric effect in AlGaN/GaN	Bykhovski et al.
1994	InGaN/AlGaN DH blue LEDs (1 cd)	Nakamura et al.
	Microwave GaN MESFET	Binari et al.
	Microwave HFET, MISFET	Binari et al.; Khan et al.
	GaN/SiC HBT	Pankove et al.
1995	AlGaN/GaN HEMT by MBE	Ozgur et al.
1996	Doped channel AlGaN/GaN HEMT	Khan et al.
	Ion-implanted GaN JFET	Zolper et al.
	340 V V_{GD} AlGaN/GaN HEMT	Wu et al.
	1st blue laser diode	Nakamura and Fosal
1997	Quantification of piezoelectric effect	Asbeck et al.
	AlGaN/GaN HEMT on SiC	Binari et al.; Ping et al.
		Gaska et al.
	1.4 W @ 4 GHz	Thibeault et al.
	0.85 W @ 10 GHz	Siram et al.
	3.1 W/mm at 18 GHz	Wu et al.
1998	3.3 W	Sullivan et al.
	p/n junction in LEO GaN	Kozodoy et al.
	HEMT in LEO GaN	Mishra et al.
	6.8 W/mm (4 W) @ 10 GHz HEMT on SiC	Sheppard et al.
	10^{-4} Hooge factor for HEMT on SiC	Levinshtein et al.
	1st AlGaN/GaN HBT	McCarthy et al.
		Ren et al.
	1st GaN MOSFET	Ren et al.
1999	9.1 W/mm @ 10 GHz HEMT on SiC	Mishra et al.
	GaN BJT (npn)	Yoshida et al.
2000	4.3 kV AlGaN rectifier	Zhang et al.
	pnp GaN/AlGaN HBT	Zhang et al.
	pnp GaN BJT	Zhang et al.

For laterally-depleting devices, the structure consisted of ~3μm of resistive (10^7ohms per square) GaN. To form ohmic contacts, Si^+ was implanted at $5x10^{14}$ cm^{-2}, 50 keV into the contact region and activated by annealing at 150°C for 10 secs under N_2. The resulting n-type carrier concentration was $1x10^{19}$ cm^{-3}. The ohmic and rectifying contact metallization was the same as described above.

Three different edge termination techniques were investigated for the planar diodes:

(i) use of a p-guard ring formed by Mg^+ implantation at the edge of the Schottky barrier metal. In these diodes the rectifying contact diameter was held constant at 124μm, while the distance of the edge of this contact from the edge of the ohmic contact was 30μm in all cases.

(ii) use of p-floating field rings of width 5μm to extend the depletion boundary along the surface of the SiO_2 dielectric, which reduces the electric field crowding at the edge of this boundary. In these structures a 10μm wide p-guard ring was used, and 1-3 floating field rings employed.

(iii)use of junction barrier controlled Schottky (JBS) rectifiers, i.e. a Schottky rectifier structure with a p-n junction grid integrated into its drift region.

In all of the edge-terminated devices the Schottky barrier metal was extended over an oxide layer at the edge to further minimize the field crowding, and the guard and field rings formed by Mg^+ implantation and 1100°C annealing.

Figure 1 (left) shows a schematic of the planar diodes fabricated with the p-guard rings, while the right of the Figure shows the influence of guard ring width on V_B at 25°C. Without any edge termination, V_B is ~2300 V for these diodes. The forward turn-on voltage was in the range 15-50 V, with a best on-resistance of $0.8\Omega m^2$. The figure-of-merit $(V_B)^2/R_{ON}$ was 6.8 $MW{\cdot}cm^{-2}$. As the guard-ring width was increased, we observed a monotonic increase in V_B, reaching a value of ~3100 V for 30μm wide rings. The figure-of-merit was 15.5 $MW{\cdot}cm^{-2}$ under these conditions. The reverse leakage current of the diodes was still in the nA range at voltages up to 90% of the breakdown value. Similar results were obtained with the field rings or JBS control.

The results shown in Figure 1 are convincing evidence that proper design and implementation of edge termination methods can significantly increase reverse breakdown voltage in GaN diode rectifiers and will play an important role in applications at the very highest power levels. For example, the target goals for devices intended to be used for transmission and distribution of electric power or in single-pulse switching in the subsystem of hybrid-electric contact vehicles are 25 kV standoff voltage, 2 kA conducting current and forward voltage drop <2% of the standoff voltage. At these power levels, it is expected that edge termination techniques will be essential for reproducible operation.

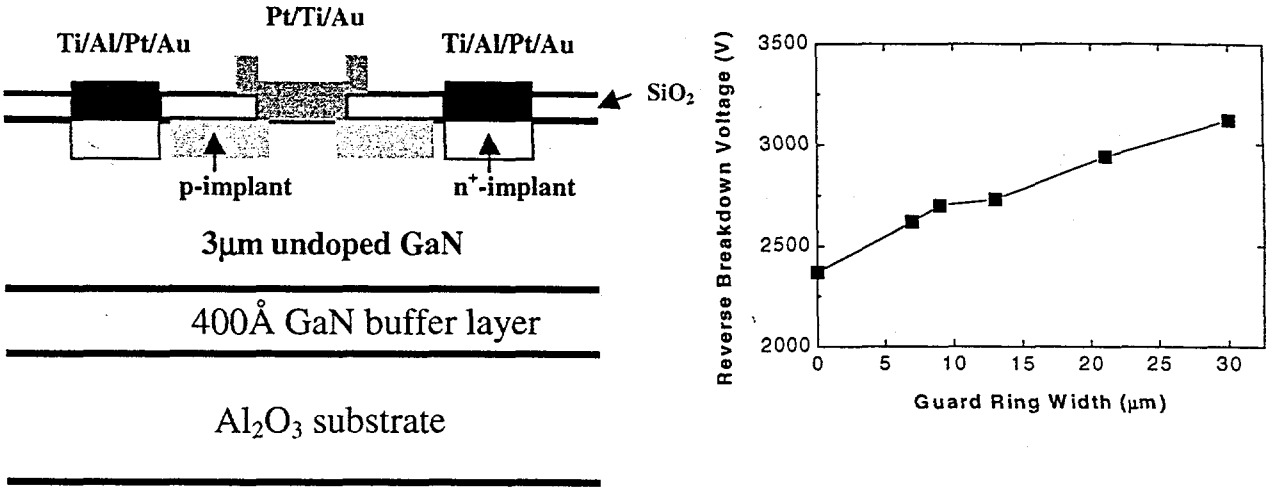

Figure 1. (left) View of rectifiers with p-type guard. (right) Variation of V_B with guard ring width.

To place our results in context with reported SiC Schottky diode performance reported in literature, Figure 2 shows a plot of specific on-resistance versus reverse breakdown voltage for SiC and GaN diodes, together with the calculated (theoretical) performance. The 3.1 kV result for GaN reported here is still well below the theoretical value, indicating that further improvement in processing and materials are needed. Some reported SiC devices have performance close to the theoretical limit, reflecting greater maturity of this technology at present.

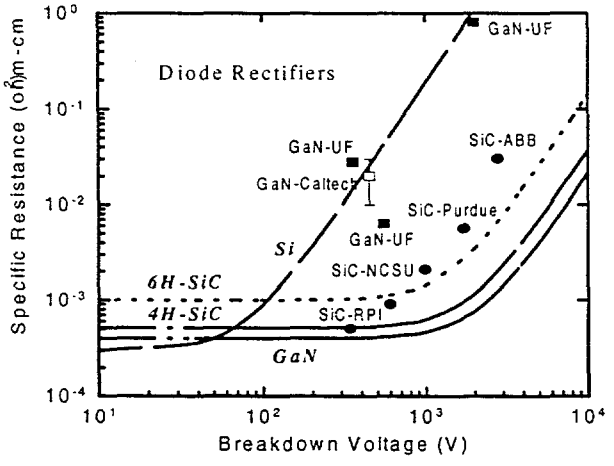

Figure 2. On-resistance versus blocking voltage for SiC and GaN diode rectifiers. The performance limits and GaN devices are shown by the solid lines.

AlGaN RECTIFIERS

The undoped $Al_xGa_{1-x}N$ layers were grown by atmospheric pressure Metal Organic Chemical Vapor Deposition at 1040°C (pure GaN) or 1100°C (AlGaN) on (0001) oriented sapphire substrates. The precursors were trimethylgallium, trimethlygaluminum and ammonia, with H_2 used as a carrier gas. The growth was performed on either GaN (in the case of GaN active layers) or AlN (in the case of AlGaN active layers) low temperature buffers with nominal thickness of 200Å. The active layer thickness was ~2.5μm in all cases and the resistivity of these films was of order $10^7\Omega$cm. To form ohmic contacts in some cases, Si^+ was implanted at $5x10^{14}$ cm^{-2}, 50 keV into the contact region and activated by annealing at 1150°C for 10 secs under N_2. The contacts were then formed by lift-off of e-beam evaporated Ti/Al/Pt/Au annealed at 700°C for 30 secs under N_2. The rectifying contacts were formed by lift-off of e-beam evaporated Pt/Ti/Au (diameter 60-1100μm). The on-resistance of the AlGaN diodes was higher than for pure GaN, due to higher ohmic contact resistance. The lowest R_{ON} achieved was $3.2\Omega cm^2$, leading to a figure-of-merit of ~5.5 $MW{\cdot}cm^{-2}$.

Figure 3 shows the variation of V_{RB} with Al percentage in the AlGaN active layers of the rectifiers. In this case we are using the V_{RB} values from diodes without any edge termination or surface passivation. The calculated bandgaps as a function of Al composition are also shown, and were obtained from the relation

$$Eg(x) = EgGaN(1-x) + EgAlN \cdot x - bx(1-x)$$

where x is the AlN mole fraction and b is the bowing parameter with value 0.96 eV. Note that V_{RB} does not increase in linear fashion with bandgap. In a simple theory V_{RB} should increase as $(Eg)^{1.5}$, but it has been empirically established that factors such as impact ionization coefficients and other transport parameters need to be considered and that consideration of Eg alone is not sufficient to explain measured V_{RB} behavior. The fact the V_{RB} increases less rapidly with Eg at higher AlN mole fractions may indicate increasing concentrations of defects that influence the critical field for breakdown.

The reverse I-V characteristics of all of the rectifiers showed $I \propto V^{0.5}$ over a broad range of voltage (50-2000 V), indicating that Shockley-Read-Hall recombination is the dominant transport mechanism. The current density in all devices was in the range $5\text{-}10x10^{-6}$ $A{\cdot}cm^{-2}$ at 2 kV. At low biases ($\leq$ 25 V) the reverse current was proportional to the perimeter of the rectifying contact, suggesting that surface contributions are the most important in this voltage range. For higher biases, the current was proportional to the area of the rectifying contact. Under these conditions, the main contribution to the reverse current is from under this contact, i.e. from the bulk of the material. It is likely that the high defect density in heteroepitaxial GaN is a primary cause of this current.

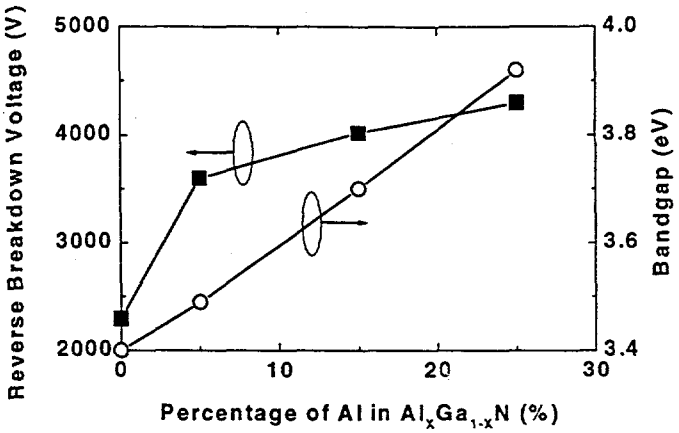

Figure 3. Variation of V_{RB} in $Al_xGa_{1-x}N$ rectifiers without edge termination, as a junction of Al concentration. The bandgaps for the AlGaN alloys are also show.

When pushed beyond breakdown, the diodes invariably failed at the edges of the rectifying contact. As described earlier, the use of metal field plate contact geometries with SiO_2 as the insulator and either guard rings or floating field rings significantly increased V_B. These rectifiers generally did not suffer irreversible damage to the contact upon reaching breakdown and could be re-measured many times.

GaN/AlGaN HETEROJUNCTION BIPOLAR TRANSISTORS

Both npn and pnp HBTs have been fabricated with emitter contact diameters in the range 50-100μm. HBT power microwave amplifiers are mostly designed on common-emitter or common-base operation. The current gain is greater than unity only in the common-emitter mode, but the common-base mode is attractive because of the possibility of appreciable power gain obtained through the impedance transformation offered by this amplifier.

In all of our devices we have observed that the saturated collector current was nearly equal to the emitter current, which indicates high emitter injection efficiency. Gummel plots showed dc current gains of 15-20 at room temperature. In many of the devices it is difficult to obtain common-emitter operation due to leakage in the collector-base junction, and at all temperatures (25-300°C) the junction ideality factors for both emitter-base and collector base junctions were close to 2, indicative of significant recombination. By removing the base contact we observed no collector current, which confirms the transistor modulation.

For npn devices the performance is limited by the high base resistnace, which originates from the deep ionization level of the Mg acceptors. In these devices we have achieved maximum current densities of 2.55 $kA \cdot cm^{-2}$ at V_{BC} = 8 V, corresponding to power densities of 20.4$kW \cdot cm^{-2}$.

There are two advantages to the pnp configuration for AlGaN/GaN HBTs. Firstly, there is a large emitter-base energy bandgap offset than in npn structures, and secondly, the base resistance will be much lower due to higher doping level achievable in n-type material. The best pnp HBTs we fabricated can be operated up to current densities of over 2kA·cm^{-2} at 25 V, corresponding to power densities above 50kW·cm^{-2}. A Gummel plot is shown in Figure 4.

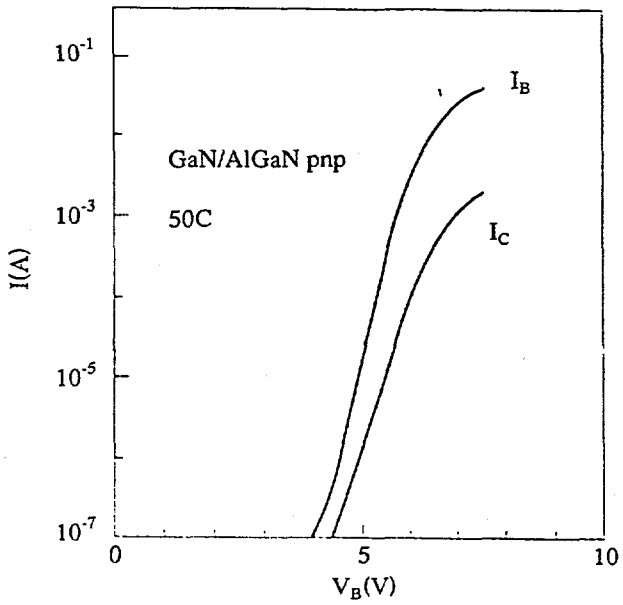

Figure 4. Gummel plot of pnp HBT with $V_{CB} = 0$.

GaN BIPOLAR JUNCTION TRANSISTORS

The epitaxial growth of BJTs is simpler than for HBTs because the emitter layer is comprised of GaN rather than AlGaN. In our npn devices we have achieved maximum current densities of 3.6kA·cm^{-2} at a collector-base voltage of 15 V, corresponding to a power density of 54kW·cm^{-2}. The maximum common-emitter dc current gain was ~15 for temperatures up to 300°C. The operation of both GaN BJTs and GaN/AlGaN HBTs was simulated using a program based on the drift-diffusion model. This simulation showed that at low current densities the HBT enjoys and advantage due to the conduction band offset, but that at higher current densities the results converged. This suggests that simple BJTs are useful as power devices.

The dc characteristics were measured up to a V_{BC} of 65 V in the common-base mode. A stable current density of 204A·cm^{-2} was run at this voltage, corresponding to a power density of 40kW·cm^{-2}. These values can clearly be increased by optimized design of the layer structure and mask layout. The devices showed little fall-off in performance at temperatures up to 250°C.

GaN METAL OXIDE SEMICONDUCTOR FIELD EFFECT TRANSISTORS

A GaN depletion-mode metal oxide semiconductor field effect transistor was demonstrated, using $Ga_2O_3(Gd_2O_3)$ as the gate dielectric, similar to the approach reported for GaAs and InGaAs. The MOS gate reverse breakdown voltage was > 35 V, significantly higher than obtained using a simple Pt Schottky gate on the same material. A maximum extrinsic transconductance of $15mS \cdot mm^{-1}$ was obtained at V_{DS} = 30 V and device performance was limited by the contact resistance. A unity current gain cut-off frequency, f_T, and maximum frequency of oscillation, f_{MAX}, of 3.1 and 10.3 GHz, respectively were measured at V_{DS} = 25 V and V_{GS} = -20 V. The device performance can be improved by optimizing the layer structure using a thin and heavily doped channel layer, which will reduce the contact resistance and enhance the transconductance.

AlGaN/GaN HEMTs

(a) dc performance. AlGaN/GaN transistor development has followed the material improvements driven by photonic devices such as LEDs and laser diodes. Table II outlines the key historical results for this technology.

The first reports of GaN based transistors were by Khan et al. with the demonstration of a GaN MESFET and an AlGaN/GaN HEMT. Both transistors had gate lengths of 4μm with the MESFET having a g_m of 23 mS/mm and I_{DS}(max) of ~180 mA/mm (@V_{GS} = 0 V, V_{DS} = 20 V). The AlGaN/GaN HEMT achieved a g_m of 28 mS/mm at 300 K (46 mS/mm at 77 K) and I_{DS}(max) of ~50 mA/mm (@V_{GS} = 0.5 V, V_{DS} = 25 V). The HEMT structure had a 2DEG mobility of 563 cm^2/V s at 300 K and 1517 cm^2/V s at 77 K. The first microwave results were published by Binari et al., for a GaN MESFET with a demonstrated f_t of 8 GHz and a f_{max} of 17 GHz for a gate length of 0.7μm.

Since the early results, significant improvements have been made in material quality and device processing. AlGaN/GaN 2DEG mobilities up to 2019 cm^2/V s have been reported for growth on 6H-SiC substrates and ~1600 cm^2/V s for growth on sapphire substrates. The saturation current has been pushed to 1.6 A/mm and the transconductance has reached 340 mS/mm.

(b) Microwave small and large signal performance. Improvements in the small signal microwave performance of AlGaN/GaN HEMTs has tracked the dc improvements. The present state-of-the-art for unity current cut-off frequency (f_t) is 75 GHz by Eastman and co-workers at Cornell University. Large signal power results for HEMT on SiC substrates include total power of 9.1 W (2-mm-wide gate) at 10 GHz with 10 dB of gain with a power density of 6.8 W/mm (4.1 W/mm at 16 GHz) measured on smaller devices. At 18 GHz a

Table II. AlGaN/GaN HFET device results in reverse chronological order (after B.E. Foutz, http://iiiv.tn.coornell.edu/www/foutz/ganhfet.html).

Gate Length	L_{SD}	f_T	f_{max}	L_{sd}	rf power	gm_{ext}
micron	micron	GHz	GHz	A/mm	W/mm at GHz	mS/mm
0.15		65	80	1.300	1.8 at 4	300
3	5			0.800		140
0.45		28	114	0.680	6.8 at 0	200
0.7	2	15	42	d 1.100	2.82 at 10	270
0.4		26	51	0.85		
1.4	3.6			0.475		220
0.15		67	140	0.700	1.55 at 3	230
0.25	2	28	40	0.750		120
0.25	2	53	58	1.430		229
0.5	2	33	41	1.400		221
1	3	15	24	1.220		205
0.7	2	17.5	44	1.050	2.84 at 8 2.57 at 10	220
0.9	2	15	35	1.000		255
0.25	2		45	1.020	1.71 at 8.4	220
1.5	5			0.950		142
0.25	1.6	52	82	1.130	3.3 at 18	240
0.2	1.6	50	92	0.806	1.7 at 10	240
0.12		46.9	103	0.550		120
0.25	2-3			1.710		222
0.25	2			1.000		130
4	6			1.000		130
2		6	11	0.260		105
0.25	2	37	81	1.000		152
0.5	2	21	53	0.880		
0.7	2	14	44	0.850		
1.0	3	11	31	0.740		122
1	3	9.6	27.2	0.700	1.57 at 4	160
1.5	3			1.100		270
0.12		46.9	103	0.560		b80
0.25	2	37.5	80.4	10.20		220
0.25	2	27	80	0.420		120
1	5	6	11	0.200		70
1.5	4			0.275		142
0.15	2	29.8	97.4	0.600	0.27 at 10	120
1	4	6	15	0.340		120
1.5	>2.5			0.695		222
1.5	3			0.330		130
1	3			0.310		140
2	4			0.490		186
1	5			.0350		120
1	5	18.3		0.600		110
0.25	>1	21.4	77.5	0.150		40
0.25	2	36.1	70.8	0.200		90
1	5			0.333		23
3	5			0.300		120
0.23	1.75	22	70	0.050		24
0.25	1.75	11	35	0.060		27
4	10			0.500		28

power density of 3.1 W/mm has been achieved on a sapphire substrate. Total power results have also been pushed up to 7.6 W achieved at 4 GHz for HEMTs grown on sapphire and flip-chip mounted on AlN carriers[9] These large signal results, however, are still not up to the level one would predict from the dc characteristics and the small signal performance of up to ~10 W/mm at 10 GHz. In some cases, the performance shortfall is evident in current and gain compression at high applied voltages. This compression is due to traps in the band gap, possibly at the surface, in the AlGaN barrier, or in the GaN buffer. Presently, the origin of the traps is still being studied, however, a similar phenomena was observed in the early GaAs device work and later overcome. In the GaAs case, the traps were due to surface states but this may not be the same in the AlGaN/GaN system.

(c) Elevated temperature performance. The group III-nitride semiconductors have been considered an ideal candidate for high temperature electronic devices due to their large band gap and resulting low thermal carrier generation rate. For this potential to be realized, defect levels in the band gap must be reduced since they will enhance undesirable dark and shunt currents. This can be seen in the temperature dependence of conduction reported by Khan et al., where a AlGaN/GaN HEMT demonstrated a large shunt current apparently resulting from defect assisted conduction in the GaN buffer layer already at 200°C. Subsequently a GaN MESFET with an improved semi-insulating buffer was shown by Binari et al., to maintain reasonable pinch-off characteristics at 400°C. When taken to 500°C, the MESFET gate electrode began to interact with the GaN surface and irreversibly degrade the transistor operation. A AlGaN/GaN HEMT has been further pushed to operate at 750°C by achieving a 1.0 eV activation energy for conduction in the buffer layer and employing a thermally stable Pt-Au gate contact. More work is needed to optimize such elevated temperature operation and device optimize such elevated temperature operation and device packaging will also need to be considered.

SUMMARY

Tremendous progress has been made in advancing the growth, processing and design of GaN power electronics in recent times. There are as yet no commercially-available devices and this may take another 3-5 years to occur.

ACKNOWLEDGMENTS

The work at the various institutions has been supported by ONR (J.C. Zolper), DARPA (D. Radack), EPRI (B. Damsky), NSF (L. Hess), by BMDO, and National Science Council of ROC. Sandia is a multiprogram laboratory operated by Sandia Corporation, a Lockheed-Martin company, for the US Department of Energy under contract No. DEAL04-94-AL85000.

REFERENCES

[1] see for example, M.S. Shur and M.A. Khan, in GaN and Related Materials II, ed. S.J. Pearton (Gordon and Breach, NY, 2000).

[2] S.C. Binari, L.B. Rowland, W. Kruppa, G. Kelner, K. Doverspike and D.K. Gaskill, Electron. Lett. 30, 1248 (1994).

[3] L.F. Eastman, K.G. Chu, J. Smart and J.R. Shealy, Mat. Res. Soc. Symp. Proc. 512, 3 (1998).

[4] S.T. Sheppard, K. Doverspike, W.L. Pribble, S.T. Allen and J.W. Palmour, 56th Device Research Conference, Charlottesville, VA, June 1998).

[5] Y.-F. Wu, B.J. Thibeault, B.P. Keller, S. Keller, S.P. DenBaars and U.K. Mishra, Topical Workshop on Heterostructure Electronics, Kanagawa, Japan, September 1998.

[6] L. Daumiller, L. Kirchner, M. Kamp, K.J. Eheling, L. Pond, C.E. Weitzel and E. Kohn, 56th Device Research Conference, Charlottesville, CA, June 1998